CrystEngComm

Accepted Manuscript

ROYAL SOCIETY OF CHEMISTRY

www.rsc.org/crystengcomm

Journal Name

RSCPublishing

COMMUNICATION

Capturing the structural diversification upon thermal desolvation of a robust metal organic frameworks via a single-crystal-to-single-crystal transformation†

Cite this: DOI: 10.1039/xoxxoooooox

Received ooth January 2012,
Accepted ooth January 2012

DOI: 10.1039/xoxxoooooox

www.rsc.org/

Sandeep Kumar[a] and Sanjay K. Mandal[a]*

Using a new mixed polypyridyl-carboxylate ligand, a 2D neutral robust framework of Zn(II), $\{[Zn(bpaipa)]\cdot DMF\cdot 2H_2O\}_n$ (1) (where H_2bpaipa = 5-(bis(pyridin-2-ylmethyl)amino)isophthalic acid), has been synthesized under solvothermal conditions in 71% yield. It undergoes single-crystal-to-single-crystal transformation upon thermal desolvation without a change in topology of the framework where the desolvated structure shows an orientation change of an uncoordinated carboxylate oxygen atom and the pyridyl groups of the ligand within the pores. Both structures have been determined by single crystal X-ray analysis. Its high thermal stability (>350 °C) and framework integrity towards many solvents are also demonstrated by variable temperature powder X-ray diffraction and thermogravimetric analysis.

In recent years various strategies for the rational design of metal organic frameworks (MOFs), also known as porous coordination polymers (PCPs), are evolving for their structural diversity and intriguing molecular topology and more importantly for their potential applications in the fields of gas storage, separation, catalysis, magnetism, drug delivery, etc.[1-5] One of the key features of these frameworks is having permanent porosity for demonstrating their viability in certain applications. These frameworks are constructed from a variety of metal ions/clusters (as nodes) and multitopic organic ligands (as linkers). Through judicious choice of the components in making such frameworks, it is possible in principle to generate materials with tunable structures and properties. The pore size and chemical functionality of a wide variety of open frameworks can be modulated by the nature of the linkers. Based on their synthesis via the one-pot self-assembly process under hydro-/solvothermal conditions, most of the time the available pores within the frameworks are filled with solvent molecules.[2,3] In this respect, removal or exchange of guest molecules in the host assemblies through the solid state transformations, such as single-crystal-to-single-crystal transformation, is a difficult but achievable route where the formation of a stable porous material is unique. If this structural transformation is reversible in nature, then investigation of the desolvated and resolvated species not only allows one to understand its formation but more importantly provide an opportunity to use it in various applications ranging from molecular recognition and separation to gas storage and sensing.[1c] However, the daughter crystals obtained from the desolvation/resolvation process are seldom found to be suitable for single crystal structure determination.[6-8,9a]

For our effort to contribute to this field of research, we have utilized a three-component self-assembly approach under ambient as well as hydrothermal conditions where the importance of the ancillary liagnd (mostly tri-, tetra- and hexadentate polypyridyl ligands) as well as the multitopic linkers (mostly carboxylates) are demonstrated.[9] In continuation of our work, we are now focusing on the mixed polypyridyl-carboxylate functionalities in a single organic component to temporally connect with numerous di- and trivalent metal ions. Herein, we report our effort in using a new ligand H_2bpaipa (where H_2bpaipa = 5-(bis(pyridin-2-ylmethyl)amino)isophthalic acid) to make a 2D robust neutral framework of Zn(II), $\{[Zn(bpaipa)]\cdot DMF\cdot 2H_2O\}_n$ (**1**), under solvothermal conditions. Like others, we targeted this framework for gas and vapor adsorption studies with standard pretreatment of the sample at a temperature (140 °C) close to the boiling point of the solvent under dynamic vacuum conditions for 24 h; however, preliminary but reproducible gas adsorption studies indicating much lower than expected values for nitrogen and methane (see Fig. S1, ESI†) prompted us to look into the desolvated species more carefully via single-crystal-to-single-crystal transformation for any structural change due to this pretreatment. Based on the single crystal structure of the desolvated species, $\{[Zn(bpaipa)]\}_n$ (**2**), it is clearly understood that there is no change in topology of the framework but an orientation change of an uncoordinated carboxylate oxygen atom and the pyridyl groups of the ligand within the pores has occurred reducing the available pore size. Therefore, this finding is very important in undertaking such adsorption studies, particularly when the crystal structure of the desolvated species is difficult to obtain as mentioned above and only a few reports are available in the literature;[6-8,9a] most of the time it is assumed on the basis of powder X-ray data that there is no change in the framework due to pretreatment of a sample for gas and vapor adsorption studies. We also demonstrate the high thermal stability (>350 °C) and resistance

to various organic solvents of **1** through variable temperature powder X-ray diffraction and TGA.

Compound **1** was synthesized via the solvothermal reaction of $Zn(OAc)_2{\cdot}2H_2O$ and H_2bpaipa in a mixture of DMF and water (1:1 ratio) with an excellent yield of 71%, as shown in Scheme 1 (for further details). In its FTIR spectrum (Fig. S2, ESI†), the asymmetric and symmetric stretch for the carboxylate of the ligand appear at 1633 cm^{-1} and 1345 cm^{-1}, respectively, ($\Delta\nu = \nu_{asym} - \nu_{sym} =$ 288 cm^{-1}) indicating the monodentate binding mode to Zn(II),[10] which is confirmed in its crystal structure discussed below. A peak at 1662 cm^{-1} indicates the presence of the lattice DMF molecule.

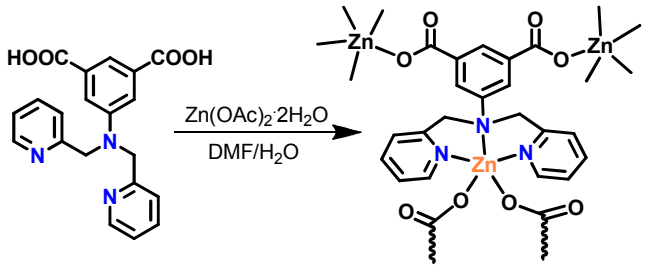

H_2bpaipa {Zn(bpaipa)]·DMF·$2H_2O$}$_n$ (**1**)

Scheme 1. Solvothermal synthesis of **1**.

Compound **1** crystallizes in the monoclinic $P2_1/n$ space group (see Table S1, ESI†).[11-14] The asymmetric unit consists of one Zn^{II}, one bpaipa ligand and lattice solvents (one molecule of DMF and two molecules of water). Thus the overall framework is neutral. As shown in Fig. S3 (ESI†), the metal lies in a distorted square-pyramidal environment formed by three nitrogens of the ligand - two pyridyl nitrogen (distances: Zn-N_{py}, 2.089(3) Å and 2.059(3) Å) and one alkyl nitrogen (distance: Zn-N_{alkyl}, 2.400(3) Å) - and two oxygens of two different carboxylates from two different ligands (distances: 2.062(2) Å and 1.989(2) Å). The degree of distortion from the ideal geometry is reflected in the bond angles around the metal center: O1"-Zn1-N3, 107.49(11)°; N2-Zn1-N3, 150.47(11)°, O1"-Zn1-N1, 130.53(10)°, etc. The τ parameter, which is an indicator[15] for the deviation from the ideal square-pyramidal (τ = 0) and trigonal bipyramidal (τ = 1) geometries for five coordinate metal centers, is found to be 0.22 for **1**. Both carboxylate groups bind in a monodentate fashion. The selected bond distances and angles for **1** are listed in Table S1. These Zn-N/O distances are very similar to those reported for MOFs with similar ligands.[16] With such metal-ligand connectivity, an overall 2D framework is formed in **1** having a pore with a dimension of 14.715(2) Å x 9.586(2) Å (defined by the distance between corner Zn^{2+} centers) as shown in Fig. 1, top. Considering the added methylpyridyl group in the H_2bpaipa ligand compared to its parent Schiff base or reduced Schiff base ligands reported by others,[16] the coordination environment of Zn^{II} in **1** is different with respect to geometry and having no coordinated solvent molecule.[16] A schematic representation of **1** without these solvent molecules (see Fig. S4, ESI†) provides the shape of the large pores - a PLATON[17] analysis shows that about 33% of the unit cell volume is occupied by the solvent molecules. Simplified topological analysis by TOPOS[18] on **1** revealed that it was a uninodal 5-c net with the Schläfli symbol {3^3.4^3.5^4} (Fig. S5, ESI†). The lattice water molecules form a zig-zag chain with the coordinated oxygens of carboxylate groups and the DMF molecules situated in the large pores as shown in its space filling representation (Fig. 1, bottom). Based on these hydrogen bonding interactions a 3D network is established in **1**. The phase-purity of the bulk **1** was studied by powder X-ray diffraction studies which showed good agreement with simulations based on the single crystal structure (see Fig. S6, ESI†).

In order to understand the thermal stability and its structural variation as a function of temperature, thermogravimetric analyses (TGA) was recorded for the single-phase polycrystalline sample of **1**. The TGA scan shown in Fig. S7 (ESI†) between 25 and 500 °C indicates that the continuous loss of all solvent molecules occurs up to 200 °C and then it is stable up to 350 °C (*vide infra*), after which subsequent decomposition of the product(s) occurs. This desolvation process (see Fig. S8, ESI†) was further followed with variable temperature FTIR data (see Fig. S9, ESI†) which suggested that a complete loss of all solvent molecules can be achieved at 170 °C based on the disappearance of the peak at 1662 cm^{-1} due to DMF. Thus, the single crystals of **1** were heated at 140 °C under dynamic vacuum conditions using a vacuum oven for 1 h.

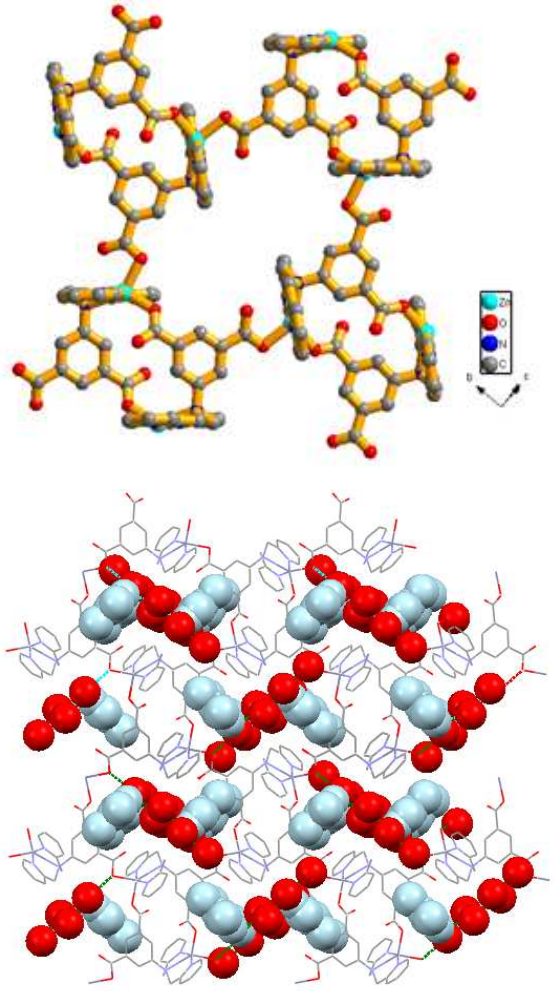

Fig. 1 Top: Crystal structure of **1** showing the large pore without the solvent molecules; hydrogen atoms are not included for clarity. Bottom: Space filling representation of **1**, where the pores are occupying the DMF and H_2O lattice solvent molecules.

A single crystal from the batch used for variable temperature FTIR experiment was chosen for the single crystal structure analysis of the desolvated species, which was confirmed to be {[Zn(bpaipa)]}$_n$ (**2**). Compound **2** also crystallizes in the monoclinic $P2_1/n$ space group (see Table S1, ESI†)[11-14] with the same asymmetric unit found in **1** except that there were no solvent molecules and thus forms a 2D framework (see Fig.

Journal Name RSCPublishing

COMMUNICATION

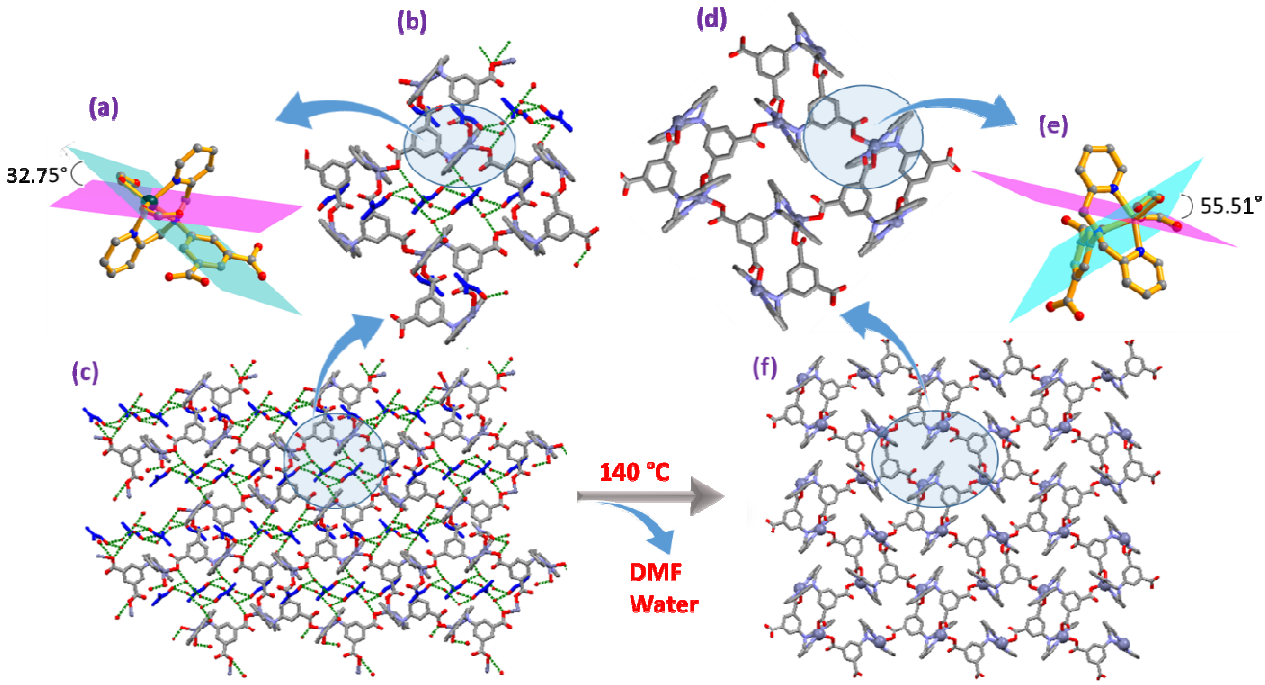

Fig. 2 Schematic representation of the desolvation process of **1** to **2**: an overall change in the network is shown in (c) and (f) while the change within the large pore due to loss of solvent molecules is shown in (b) and (d) and the change around the metal centers is shown in (a) and (e).

S10, ESI†). However, there are noticeable changes in the unit cell parameters and volume in **2** compared to **1**. While the length of both b and c axes was shortened by 2 Å in each case, the value of β increased by 2.3˚. And, the reduction of unit cell volume (567.3 Å^3; 24.7%) at 100 K (similar values are obtained at 200 K and 296 K) is much more than expected for the loss of four DMF and eight water molecules per unit cell. This is unexpected unless there are other changes occurred due to the desolvation process. Such an event with a 24.7% reduction in cell volume can be compared to a relevant case[7d] with 35.1% reduction in cell volume.

This can be understood if the overall change of the framework shown in Fig. 2 (c and f) is carefully considered. With a close-up view (Fig. 2, b and d) of the pores in **1** and **2**, it is clear that the change in positions of uncoordinated oxygen O2 of a carboxylate group and one of the pyridyl groups (with that containing N2) of the ligand are the effects of the desolvation process. This has caused a change around the metal center which is reflected by a large shift in the angle between the planes defined by the metal center and carboxylate groups in the ligand (32.75(3)˚ in **1** and 55.51(3)˚ in **2**), as shown in Fig. 2, a and e. Like **1**, Zn^{II} in **2** lies in a distorted square-pyramidal environment formed by three nitrogens of the ligand - two pyridyl nitrogen and one alkyl nitrogen - and two oxygens of two different monodentate carboxylates from two different ligands. The τ parameter is found to be 0.15 for **2**. Comparing the bond distances and angles around Zn^{II} for **2** (listed in Table S2, ESI†) with those for **1**, it can be noted that except one of the Zn-Npy (Zn1-N2) distance (the one which moved further inwards the pore) which lenthened by 0.06(2) Å, all other distances become shorter by 0.05(2)-0.06(2) Å in **2**. For the same reason, angles involving carboxylate oxygen O1 (the other oxygen in this group is O2) and pyridyl nitrogen N2 are affected the most. Upon further consideration of this structural change as shown in Fig. 3, it can be seen that the O2 atom is moved inward the pore for the conversion of **1** to **2** (the O2···O2' distance: 9.002(2) Å in **1** vs 6.901(2) Å in **2**). This has resulted in the pore accessibility less in **2** compared to **1** even though the pore dimension in **2** is 15.565(2) Å x 8.72(2) Å (based on the distance between corner Zn^{2+} centers, as was done for **1**). The topology of the framework in **2** remained the same as that of **1** (see Fig. S11, ESI†).

Based on the distinct thermal behavior, compound **1** was further investigated to provide insight into its crystalline properties at different temperatures (with a profile from 25 °C to 350 °C and then cooling back to 25 °C). As can be seen from Fig. 4 where the patterns for each step are found to be similar except a small change due to loss of solvent molecules, compound **1** retains its crystallinity and overall structure up to 350 °C which corroborates well with the thermogravimetric analysis.

In order to demonstrate the stability of **1** in different organic solvents, six sets of crystals of **2** generated through the desolvation of **1** as described above and confirmed by its TGA were immersed in different solvents (acetonitrile, dichloromethane, hexane, methanol, tetrahydrofuran and toluene) for two days and filtered to obtain the various solvates of **1**. As can be seen from Fig. 5, the PXRD patterns of all these solvates are similar to each other and match well with that of **1**. This confirms that the framework in **1** is robust enough to undergo such desolvation/resolvation process without losing its crystallinity. The TGA data (Fig. S12, ESI†) for four solvates indicate that methanol has been absorbed the most (2.5 molecules) while toluene the least (0.14 molecule), per molecule of the framework. This observation will be exploited to undertake other host-guest chemistry in future.

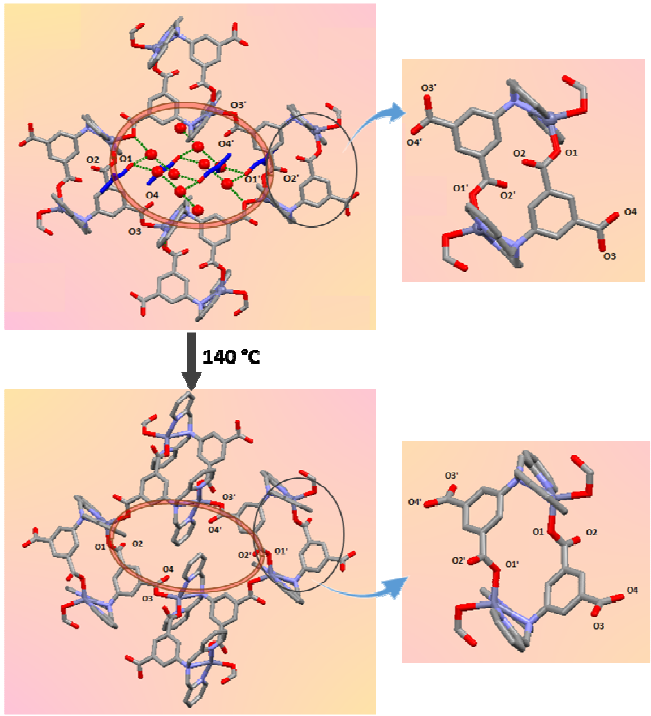

Fig. 3 Change in orientation of an oxygen atom (O2) of the carboxylate group and pyridyl groups of the ligand within the pore during the desolvation of **1** to **2**. Symmetry codes for equivalent positions are: ' = -x, -y+1, -z+2 for **1** and ' = -x, -y, -z+1 for **2**.

In conclusion, we have designed and synthesized a new mixed polypyridyl-carboxylate ligand, 5-(bis(pyridin-2-ylmethyl)amino)-isophthalic acid to construct a 2D neutral robust framework of Zn(II), $\{[Zn(bpaipa)].DMF.2H_2O\}_n$ (**1**), under hydrothermal conditions. Upon thermal desolvation of **1** via a single-crystal-to-single-crystal transformation without the loss of framework topology, the resulting structure shows an orientation change of an oxygen atom through the rotation of coordinated carboxylate groups and one of the pyridyl groups within the pores. Based on the PXRD and TGA data, the parent compound shows high thermal stability and appears to be stable in different organic solvents. Further development of several new derivatives of **1** to study their gas/vapor adsorption and sensing applications is in progress.

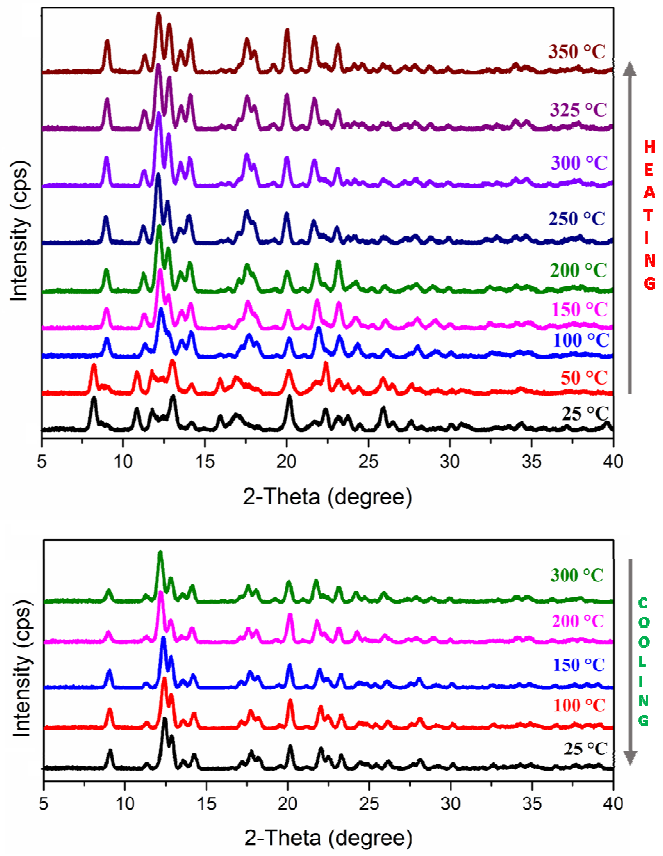

Fig. 4 Variable temperature powder diffraction patterns (top: heating from 25 °C to 350 °C; bottom: cooling back to 25 °C) indicating retention of crystallinity in **1** (due to loss of lattice solvents) up to 350 °C.

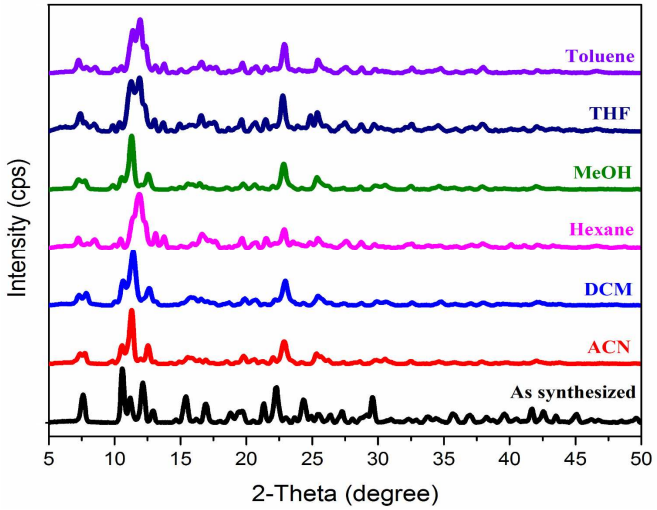

Fig. 5 PXRD patterns for the various solvates of **1**.

Acknowledgements

Sandeep Kumar is grateful to MHRD, India for a research fellowship. Authors would like to thank Dr. Sadhika Khullar for conducting the gas adsorption study and providing critical review of the manuscript. Funding for this work was provided by IISER, Mohali. The X-ray and NMR facilities at IISER, Mohali are gratefully acknowledged.

Experimental section

Synthesis of H_2bpaipa

In step 1, *5-((pyridin-2-ylmethyl)amino)isophthalic acid* was prepared with some modifications in the reported procedure.[19] To a methanolic solution of 5-aminoisophthalic acid (1.81 g (10 mmol) in 10 mL methanol) in a 50 mL RBF, triethylammine (2 mL) was added and stirred for 15 min. Subsequently, 2-pyridinecarboxyaldehyde (0.98 mL, 10 mmol) was added and stirred for 8 h. An excess of sodium borohydride (2 eqvs.) was added slowly to the above solution at 0 °C and stirred for another 10 h. Upon evaporation of most of the solvent using reduced pressure, the resulting slurry was poured into 20 mL ice cold water followed by addition of a few drops of acetic acid to make the pH 5-6. A yellowish white precipitate (1.35 g, 52%) was isolated after evaporation of the solvent. Its melting point and ^{1}H NMR data were matched with the literature values, confirming its identity and purity. This was used in the next step without any purification.

In step 2, to an aqueous solution (8 mL) of the reduced Schiff base obtained in step 1 (0.5 g, 0.002 mol), picolylchloride hydrochloride (0.32 g, 0.002 mol) was added and the mixture was stirred for 5 mins. After adding a sodium hydroxide solution (0.16 g in 1 mL water) dropwise over a period of 20 mins, the mixture was stirred for 24 h at room temperature. The aqueous reaction mixture was washed 3-4 times with chloroform followed by the addition of 1 mL dil. HCl. A yellowish solid was formed. Further work-up to remove NaCl using dry MeOH provided the desired product. Yield: 583 mg (85%). See Scheme S1, Figures S13 and S14, ESI†. ^{1}H NMR (D_2O): δ 8.33 (d, 2H), 7.65 (d, 2H), 7.48 (s, 1H), 7.21 (d, 2H), 7.19 (d, 2H), 4.76 (s, 4H). ^{13}C NMR (D_2O): δ 169.03, 152.29, 147.27, 146.13, 141.94, 131.88, 126.06, 125.23, 121.90, 118.39, 52.26. HRMS (ESI-TOF): m/z calcd for M + H^+, 364.1252; found, 364.1284.

Synthesis of $\{[Zn(bpaipa)]\cdot DMF\cdot 2H_2O\}_n$ (1)

A mixture of $Zn(OAc)_2\cdot 2H_2O$ (22 mg, 0.1 mmol), and H_2bpaipa (36.3 mg, 0.1 mmol) in DMF/H_2O (1 mL/1 mL) was heated in a 5 mL capacity Teflon lined stainless-steel reactor at 120 °C for 48 h and then cooled to room temperature in 24 h. Colorless block-shaped crystals were collected via filtration and washed with a 1:1 mixture of acetonitrile and toluene to remove the acetic acid by-product followed by drying in air. Yield 71% (38 mg) based on Zn^{2+} ion. Anal. Calc. (%) for $C_{20}H_{17}N_3O_5Zn$ (MW 444.75): C, 54.01; H, 3.85; N, 9.45. Found: C, 53.85; H, 3.80; N, 9.15. Selected FTIR peaks (KBr, cm^{-1}): 3344 (br), 1662(m), 1633(s), 1607(s), 1567(s), 1443(s), 1345(s), 1297(m), 783(m), 725(m).

Electronic Supplementary Information (ESI) available: crystallographic data [CCDC 1405287-1405288]. Scheme 1, Figures S1-S13 and Tables S1-S2. See DOI: 10.1039/c000000x/

Notes and references

[a]Department of Chemical Sciences, Indian Institute of Science Education and Research, Mohali, Sector 81, Manauli PO, S.A.S. Nagar, Mohali (Punjab) 140306, INDIA

1 (a) J. L. C. Rowsell and O. M. Yaghi, Angew. Chem., Int. Ed., 2005, **44**, 4670; (b) X. Lin, J. Jia, X. Zhao, K. M. Thomas, A. J. Blake, G. S. Walker, N. R. Champness, P. Hubberstey and M. Schröder, Angew. Chem., Int. Ed., 2006, **45**, 7358; (c) S. Kitagawa, R. Kitaura and S. Noro, *Angew. Chem. Int. Ed.,* 2004, **43**, 2334.

2 See the issue No. 5 of the 38th volume of the *Chem. Soc. Rev.* (2009).

3 See the issue No. 2 of the 112th volume of the *Chem. Rev.* (2012).

4 Representative examples: (a) R. E. Morris, *Nature Chem.,* 2011, **3**, 347; (b) J. R. Li and H. C. Zhou, *Nature Chem.,* 2010, **2**, 893; (g) R. Makiura, S. Motoyama, Y. Umemura, H. Yamanaka, O. Sakata and H. Kitagawa, *Nature Materials*, 2010, **9**, 565; (c) S. S. Y. Chui, S. M. F. Lo, J. P. H. Charmant, A. G. Orpen and I. D. Williams, *Science*, 1999, **283**, 1148.

5 Representative examples: (a) K. C. Stylianou, J. Rabone, S. Y. Chong, R. Heck, J. Armstrong, P. V. Wiper, K. E. Jelfs, S. Zlatogorsky, J. Bacsa, A. G. McLennan, C. P. Ireland, Y. Z. Khimyak, K. M. Thomas, D. Bradshaw and M. J. Rosseinsky, *J. Am. Chem. Soc*., 2012, **134**, 20466; (b) K. L. Mulfort and J. T. Hupp, *J. Am. Chem. Soc*., 2007, **129**, 9604; (c) B. Chen, C. Liang, J. Yang,D. S. Contreras, Y. L. Clancy, E. B. Lobkovsky, O. M. Yaghi and S. Dai, *Angew. Chem., Int. Ed*., 2006, **45**, 1390; (d) M. Eddaoudi, J. Kim, N. Rosi, D. Vodak, J. Wachter, M. O'Keeffe and O. M. Yaghi, *Science*, 2002, **295**, 469.

6 (a) R. Sen, D. Saha, S. Koner, P. Brandao and Z. Lin, *Chem. Eur. J.*, 2015, **21**, 5962. (b) D. L. Reger, D. M. Smith, G. J. Long, and F. Grandjean, *Inorg. Chem.,* 2011, **50,** 686; (c) D. L. Reger and M. D. Smith, *Inorg. Chem.,* 2011, **50**, 11754; (d) A. Aijaz, P. Lama and P. K. Bharadwaj, *Inorg. Chem.*, 2010, **49**, 5583; (e) C.-C. Wang, C.-T. Yeh, K.-Yi. Cheng, P.-C. Chand, M.-L. Hp, G.-H. Lee, H.-S. Shih and H.-S. Sheu, *Inorg. Chem.,* 2011, **50**, 597; (f) A. Michaelides and S. Skoulika, *Cryst. Growth Des*., 2005, **5**, 529.

7 (a) H. Li, M. Eddaoudi, M. O'Keeffe, O. M. Yaghi, *Nature*, 1999, **402**, 276; (b) C. J. Kepert and M. J. Rosseinsky, *Chem. Commun.*, 1999, 375; (c) D. Bradshaw, J. E. Warren and M. J. Rosseinsky, *Science*, 2007, **315**, 977; (d) M. P. Suh, J. W. Ko and H. J. Choi, *J. Am. Chem. Soc.*, 2002, **124**, 10976.

8 (a) T. K. Maji, K. Uemura, H.-C. Chang, R. Matsuda and S. Kitagawa, *Angew. Chem., Int. Ed.*, 2004, 43, 3269; (b) C.-D. Wu and W.-B. Lin, *Angew. Chem., Int. Ed.*, 2005, **44**, 1958; (c)

9 (a) S. Khullar and S. K. Mandal, *Cryst. Growth Des.,* 2012, **12**, 5329; (b) S. Khullar and S. K. Mandal, *Cryst. Growth Des.,* 2013, **13**, 3116; (c) S. Khullar and S. K. Mandal, *CrystEngComm,* 2013, **15**, 6652; (d) S. Khullar, V. Gupta and S. K. Mandal, *CrystEngComm,* 2014, **16**, 5705; (e) S. Khullar and S. K. Mandal, *Cryst. Growth Des.,* 2014, **14**, 6433; (f) S. Khullar and S. K. Mandal, *RSC Advances,* 2014, **4**, 39204.

10 (a) G. B. Deacon, R. J. Phillips, *Coord. Chem. Rev*., 1980, **33**, 227; (b) K. Nakamoto, *Infrared and Raman Spectra of Inorganic and Coordination Compounds, 5th Edition,* John Wiley and Sons: New York, 1997.

11 Crystal data for **1** and **2** that were collected with the use of a Bruker Kappa APEX II diffractometer equipped with a CCD detector and sealed-tube monochromated MoKα radiation (λ = 0.071073 Å) are as follows. For **1**: $C_{23}H_{26}N_4O_7Zn$, M_r = 535.85, T = 100 K, Monoclinic $P2_1/n$, a = 8.7542(8) Å, b = 16.4242(15) Å, c = 15.9879(15) Å, α = 90°, β = 91.709(2)°, γ = 90°, V = 2297.7(4) Å^3, Z = 4, D_c = 1.549 gcm^{-3}, μ = 1.122 mm^{-1}, R_{int} = 0.0467, final R_1 = 0.0443, wR_2 = 0.1123 for 3076 unique reflections (I > 2σ). For **2**: $C_{20}H_{15}N_3O_4Zn$, M_r = 426.72, T = 100 K, Monoclinic $P2_1/n$, a = 8.485(5) Å, b = 14.529(9) Å, c = 14.073(8) Å, α = 90°, β = 94.11(3)°, γ = 90°,V = 1730.4(17) Å^3, Z = 4, D_c = 1.638 gcm^{-3}, μ = 1.454 mm^{-1}, R_{int} = 0.138, final R_1 = 0.0817, wR_2 = 0.1894 for 1399 unique reflections (I > 2σ). Full details are summarized in Table S1.

12 *APEX2*, *SADABS and SAINT*; Bruker AXS inc: Madison, WI, USA, 2008.

13 G. M. Sheldrick, *Acta Crystallogr. Sect. A*, 2008, **64**, 112.

14 C. F. Macrae, I. J. Bruno, J. A. Chisholm, P. R. Edginton, P. McCabe, E. Pidocck, L. Rodriguez-Monge, T. Taylor, J. Van de Streek, P. A. Wood, *J. Appl. Cryst.,* 2008, **41**, 466.

15 A. Addison, T. Rao, J. Reedijk, J. van Rijn, G. Verschoor, *J. Chem. Soc., Dalton Trans*. **1984**, 1349.

16 (a) H.-W Kuai, X.-C. Cheng L.-D. Feng and X.-H. Zhu, *Anorg. Allg. Chem.*, 2011,**11**,1560; (b) X.-C. Cheng, X.-Hong, H.-W. Kuai, *Anorg. Allg. Chem.*, 2013, **68**, 1007; (c) X. Liu, M. Oh and M. S. Lah, *Cryst. Growth Des.*, 2011, **11**, 5064.

17 A. L. Spek, PLATON, Version 1.62, University of Utrecht, 1999.

18 Blatov, V. A.; Shevchenko, A. P.; Serezhkin, V. N. *J. Appl. Crystallogr.* 2000, **33**, 1193. TOPOS software is available for download at http://www.topos.ssu.samara.ru.

19 M. C. Das and P. K. Bharadwaj, *J. Am. Chem. Soc.*, 2009, **131**, 10942.

Art work and Synopsis

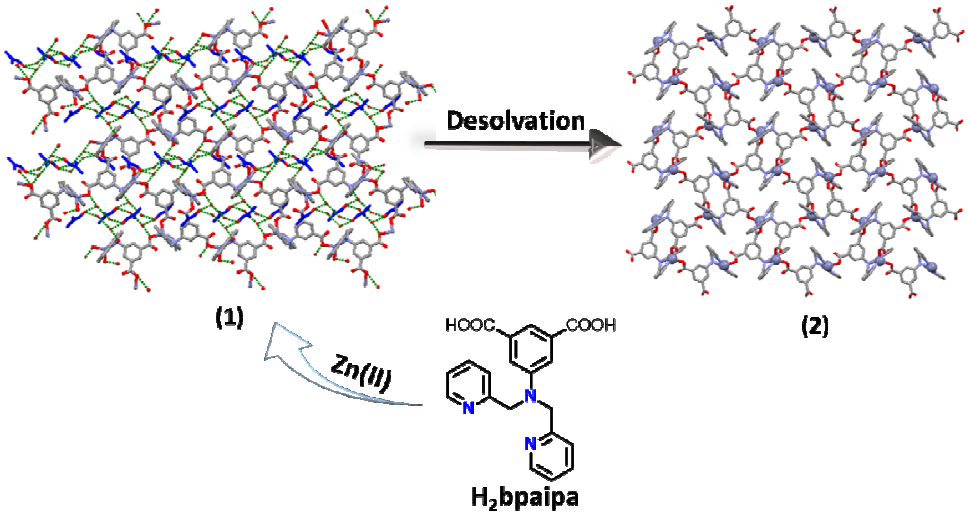

Using a robust 2D metal organic framework $\{[Zn(bpaipa)]\cdot DMF\cdot 2H_2O\}_n$(**1**), structural diversification due to thermal desolvation is captured via single-crystal-to-single-crystal transformation based on the X-ray crystallography, FTIR and TGA.